Proposal of Position Reconstruction with Polynomial Fitting Approach for Precise Motion Control

Hongzhong Zhu * **Hiroshi Fujimoto** ** **Toshiharu Sugie** ***

* *Department of Electrical Engineering, The University of Tokyo, Tokyo, Japan (e-mail: zhu@hflab.k.u-tokyo.ac.jp).*
** *Department of Electrical Engineering, The University of Tokyo, Tokyo, Japan (e-mail: fujimoto@k.u-tokyo.ac.jp)*
*** *Graduate School of Informatics, Kyoto University, Kyoto, Japan (e-mail: sugie@i.kyoto-u.ac.jp)*

Abstract: Optical encoders are extensively used for position measurements in motion control systems. The inherent quantization feature of encoders limits the control performance in many applications. This paper shows a way to reconstruct the smooth position signal from the quantized measurements. The method uses a polynomial fitting approach where the degree of polynomial is automatically selected via a convex optimization method. In addition, the information of the plant is exploited by combining an observer. The effectiveness of the proposed method is verified by simulations and experiments using a high-precision linear stage.

Keywords: quantization, optical encoder, motion control, polynomial fitting approach, convex optimization, moving horizon manner.

1. INTRODUCTION

Accurate position signals are required for high-precision control of many mechanical systems, such as NC machine tools, industrial robots, storage devices, and so on. Optical encoders, due to their easy implementation and simple construction, are extensively used for position measurements. However, as the encoder cannot reflect the actual position continuously but outputs the quantized signal, there is measurement inaccuracy in position output. The measurement error, which is also referred as the quantization error, would result in limit cycle oscillation of the systems and significantly degrade the control performance (Devasia et al., 2007). In order to relax the problem, a simple way is to use higher-resolution encoders. However, it would not only greatly increase the implementation cost, the quantization effects can also not be completely reduced as well. Therefore, understanding and suppressing the quantization effects have attracted a great deal of attention (Sur and Paden, 1998; Franklin et al., 1998).

A lot of literature can be found on reducing the quantization effects by reconstructing the position information from the encoder information. These methods usually exploit observer techniques (Tesch and Lorenz, 2008; Zhang and Fu, 2008) or Kalman filters (Luong-Van et al., 2004; Belanger et al., 1998) to estimate the position information. The methods have the potential to achieve precise state estimation for they take advantage of the system information. However, it should be noticed that most of the observer-based methods do not consider the input disturbance, which may be difficult to apply in many practical situations. On the other hand, the methods based on Kalman filters usually make the assumption that the quantization error is Gaussian noise. However, quantization error behaves as highly colored noise and these methods are not always effective.

Several other approaches devote efforts to reconstruct the output based on curve fitting techniques. The idea is usually based on the assumption that the system output can locally be approximated by low-degree polynomials. The other variables of the system, such as velocity and acceleration, can be estimated by calculating the first and second order derivative of the polynomials (Merry et al., 2010). The methods can achieve a smooth and precise reconstruction signal if the quantization step is small and the position signal is simple enough to be fitted by low-degree polynomials. However, the effectiveness is limited when high-degree polynomial becomes necessary.

Since the model-based methods share the feature of providing good estimation performance and polynomial fitting methods can achieve a smooth reconstruction signal, a polynomial fitting approach based on ℓ_1-norm regularization and observer is exploited to reconstruct the real position signal. Part of the idea is also considered in (Zhu and Sugie, 2012) for estimating the velocity information from the quantized measurements. However, the quantization effects on position control, such as the limit cycle oscillation phenomenon, are not studied. Moreover, in order to obtain a good velocity estimation, the input disturbance is assumed to be zero-mean in (Zhu and Sugie, 2012), which may not suitable in practical situations. In this paper, we also take the disturbance into account to make the reconstruction approach more applicable.

This paper is organized as follows. In Section 2, the system model is introduced, and the problem setting is described.

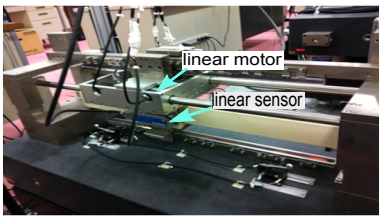

Fig. 1. Experimental setup.

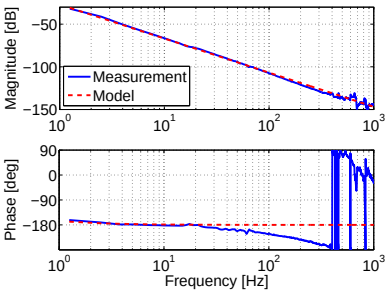

Fig. 2. Frequency characteristics.

Section 3 presents the polynomial fitting approach combined with some constraint conditions. Section 4 and 5 demonstrate the effectiveness of the proposed approach by simulations and experiments. The conclusions are summarized in Section 6.

2. POSITIONING SYSTEM AND QUANTIZATION MODEL

2.1 Positioning system

Fig. 1 shows the experimental high-precision stage. The stage is driven by linear motors located at the both sides of the carrier. An air guide system is attached to the system to reduce the non-linear friction effects. An ultrahigh precise linear scale whose resolution is 1 nm/pulse is implemented to measure the stage position. The control input is the motor currents and the output is the position. DSP(TMS320C6713, 225MHz) is used as the processor to implement the controllers. Fig. 2 shows the frequency characteristics of the Stage. The blue solid lines show the experimental measurement. The stage is modeled as

$$\dot{\boldsymbol{x}}_p(t) = \boldsymbol{A}_p\boldsymbol{x}_p(t) + \boldsymbol{B}_p(u(t) + w(t)), \quad (1)$$
$$y(t) = \boldsymbol{C}_p\boldsymbol{x}_p(t), \quad (2)$$

where

$$\boldsymbol{A}_p = \begin{bmatrix} 0 & 1 \\ 0 & -1.6327 \end{bmatrix}, \quad \boldsymbol{B}_p = \begin{bmatrix} 0 \\ 1.7959 \end{bmatrix}, \quad \boldsymbol{C}_p = [\,1\ 0\,],$$

y is the position, $\boldsymbol{x}_p := [y\ \dot{y}]^T$ is the state vector, u is the current input, and w is the input disturbance. The dotted red lines in Fig. 2 show the frequency characteristics of the model. Assume that w can be expressed by the state equation

$$\dot{x}_d(t) = \Gamma x_d(t)$$
$$w(t) = H x_d(t),$$

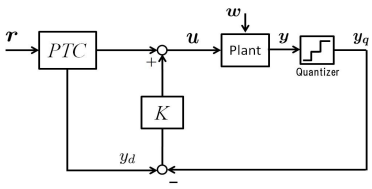

Fig. 3. Block diagram of linear stage control system.

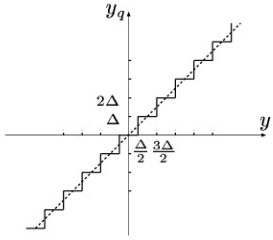

Fig. 4. Quantization characteristic. Δ is the resolution.

where $x_d \in R$ is the disturbance state, Γ, H are matrices of suitable dimensions. Denote $\boldsymbol{x} = [\boldsymbol{x}_p^T\ x_d]^T$, the augmented state equation can be expressed by

$$\dot{\boldsymbol{x}}(t) = \boldsymbol{A}\boldsymbol{x}(t) + \boldsymbol{B}u(t), \quad (3)$$
$$y(t) = \boldsymbol{C}\boldsymbol{x}(t), \quad (4)$$

where

$$\boldsymbol{A} = \begin{bmatrix} \boldsymbol{A}_p & \boldsymbol{B}_p H \\ \boldsymbol{0} & \Gamma \end{bmatrix}, \ \boldsymbol{B} = \begin{bmatrix} \boldsymbol{B}_p \\ 0 \end{bmatrix}, \ \boldsymbol{C} = [\,\boldsymbol{C}_p\ 0\,].$$

For discrete-time implementation with fixed sampling period T_s, augmented system equations (3) and (4) can be expressed as

$$\boldsymbol{x}[k+1] = \boldsymbol{A}_d\boldsymbol{x}[k] + \boldsymbol{B}_d u[k], \quad (5)$$
$$y[k] = \boldsymbol{C}_d\boldsymbol{x}[k], \quad (6)$$

where k is the discrete time index, $\boldsymbol{A}_d = e^{\boldsymbol{A}T_s}$, $\boldsymbol{B}_d = \int_0^{T_s} e^{\boldsymbol{A}(T_s-t)}\boldsymbol{B}dt$, and $\boldsymbol{C}_d = \boldsymbol{C}$.

A 2-DoF controller is exploited to control the stage, and the block diagram of the control system is shown in Fig. 3. The feedforward controller, designed by perfect tracking control (PTC) method (Fujimoto et al., 2001), is the stable inverse system of the nominal plant so that perfect tracking at every sampling instant can be theoretically guaranteed. The feedback controller is designed as a PID compensator given by

$$K = k_p + k_d\frac{s}{0.004s+1} + k_i\frac{1}{s}, \quad (7)$$

where $k_p = 2065.6$, $k_i = 34624$, $k_d = 43.45$, the bandwidth of the close-loop system is 10 Hz. The control system is discretized with the sampling period $T_s = 5$ ms.

2.2 Problem establishment

Denote Δ as the resolution of an encoder, and y_q as the quantized output, the following uniform quantization model is exploited:

$$y_q = \boldsymbol{Q}(y) = i\cdot\Delta, \quad y \in ((i-0.5)\Delta\ ,\ (i+0.5)\Delta], \quad (8)$$

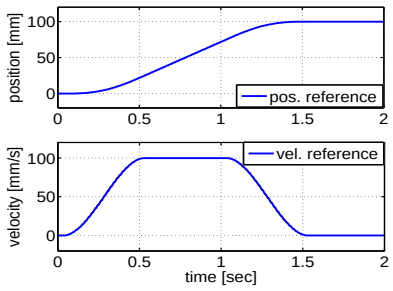

Fig. 5. Position reference and velocity reference.

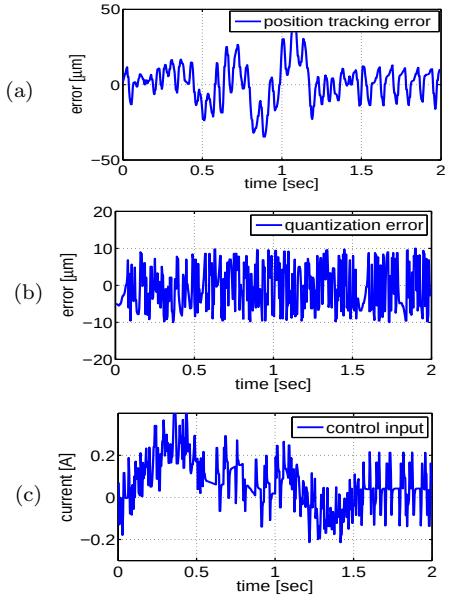

Fig. 6. Experimental results of the conventional method that the quantized measurements used for feedback. (a) shows the position tracking error. (b) shows the quantization error, and (c) shows the control input.

where $i \in Z$, the function $\boldsymbol{Q}(\cdot)$ represents the operation of quantization. Assuming the quantization range is infinite, the relationship between y and y_q is shown in Fig. 4. Note that the difference between the system output y and the measured quantized output y_q, denoted as $\xi := y - y_q$, is bounded by

$$|\xi| \leq \frac{\Delta}{2}. \tag{9}$$

In order to evaluate the effects of quantization, an encoder with the resolution of $\Delta = 20\,\mu$m is supposed to be used, as shown in Fig. 3. A software quantizer is introduced to re-quantize the position signal measured by the linear scale. An experiment including acceleration, uniform motion, deceleration and settling motion is performed. Fig. 5 shows the trajectory reference. The experimental results are shown in Fig. 6. Fig. 6(a), (b) and (c) show the position tracking error between y_d and y, the quantization error between y and y_q, and the control input u, respectively. It is observed that the limit cycle oscillation is excited so that the control performance is deteriorated, especially at the settling motion area. Moreover, the control input also behaves wildly due to the feedback signal is nonsmooth.

In order to suppress the quantization effects, high-resolution encoders are usually considered. However, it greatly increases the implementation cost. In this study, a curve fitting approach is proposed to reconstruct the real position from the quantized measurements. Since the true system output y should be smooth and band limited due to the system dynamics, it is possible to get more precise information on $y[k]$ from the past quantized measurement series $y_q[i]$ $(i \leq k)$. In the next section, we utilize the moving horizon polynomial fitting approach (Zhu and Sugie, 2012) and an observer technique to reconstruct the position measurements.

3. MOVING HORIZON POLYNOMIAL FITTING APPROACH

In this section, firstly, the quantized measurements are locally fitted by a polynomial based on the ℓ_1-norm regularization. Then, the moving horizon manner is applied for the real-time output reconstruction. Finally, several constraint conditions are derived to improve the fitting accuracy by taking into account the quantization feature and the observer technique.

3.1 Polynomial fitting formulation

A polynomial for fitting the latest $p+1$ quantized measurements $(\{y_q[k-i]\}_{i=0,1,\cdots,p})$ is considered. Here, k denotes the current time instant. In order to do so, first, choose the time interval $[a,\ b]$ in advance, and introduce the virtual time indices $\{t_i\}_{i=0,1,\cdots,p}$, which are defined by

$$t_0 = a, t_1 = a + h, \cdots, t_i = a + ih, \cdots, t_p = b,$$

where $h = (b-a)/p$. Then the data $(t_i, y_q[k-p+i])_{i=0,1,\cdots,p}$ are fitted in Euclidean space with a polynomial

$$g_k(t) = \alpha_0 + \alpha_1 t + \alpha_2 t^2 + \cdots + \alpha_m t^m,\ t \in [a\ \ b] \tag{10}$$

where $\alpha_0,\ \alpha_1,\ \cdots\ \alpha_m$ are the coefficients, and m is the degree of the polynomial. Without loss of generality, m is assumed to be $m \leq p+1$. The fitting problem is formulated by

$$\underset{\boldsymbol{\alpha}}{\text{minimize}}: \left\| \begin{bmatrix} g_k(t_0) - y_q[k-p] \\ \vdots \\ g_k(t_i) - y_q[k-p+i] \\ \vdots \\ g_k(t_p) - y_q[k] \end{bmatrix} \right\|_2^2 + \eta\|\boldsymbol{\alpha}\|_1, \tag{11}$$

with variable $\boldsymbol{\alpha} := [\alpha_0\ \alpha_1\ \cdots\ \alpha_m]^T$, and η is the weighting factor. This is an ℓ_1-norm regularization problem, and can be expressed as

$$\underset{\boldsymbol{\alpha}}{\text{minimize}}: \quad \|\boldsymbol{T}\boldsymbol{\alpha} - \boldsymbol{\beta}\|_2^2 + \eta\|\boldsymbol{\alpha}\|_1, \tag{12}$$

where

$$\boldsymbol{T} = \begin{bmatrix} 1 & t_0 & t_0^2 & \cdots & t_0^m \\ 1 & t_1 & t_1^2 & \cdots & t_1^m \\ \vdots & \vdots & \vdots & \ddots & \vdots \\ 1 & t_i & t_i^2 & \cdots & t_i^m \\ \vdots & \vdots & \vdots & \ddots & \vdots \\ 1 & t_p & t_p^2 & \cdots & t_p^m \end{bmatrix},\ \boldsymbol{\beta} = \begin{bmatrix} y_q[k-p] \\ y_q[k-p+1] \\ \vdots \\ y_q[k-p+i] \\ \vdots \\ y_q[k] \end{bmatrix}.$$

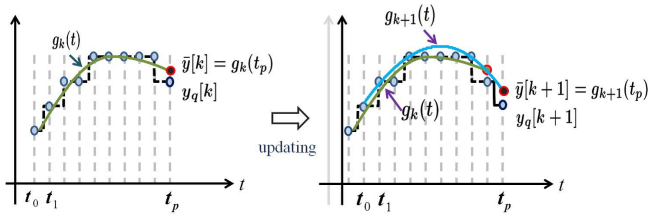

Fig. 7. Fitting strategy and updating strategy. A new polynomial should be calculated when the time instant is updated.

ℓ_1-norm introduced in (12) is used for reducing the number of non-zero elements of $\boldsymbol{\alpha}$. In this way, the unnecessary terms of the polynomial (10) can be removed automatically if a high-degree polynomial is used to fit a low-degree signal. In practical situation, m can be assigned to be relative large so that simple signal as well as complex signal can be properly fitted.

3.2 Moving horizon manner

The polynomial (10) can be determined when the convex optimization problem (12) is solved. The quantity $\bar{y}[k]$ given by

$$\bar{y}[k] := g_k(t_p) = \alpha_0 + \alpha_1 t_p + \alpha_2 t_p^2 + \cdots + \alpha_m t_p^m, \quad (13)$$

is regarded as the reconstruction value of the system output $y[k]$. Suppose that the time instant k is updated, say, from k to $k+1$, a new quantized measurement $y_q[k+1]$ is sampled. Therefore, a new polynomial $g_{k+1}(t)$ can be determined by fitting the data $\{y_q[k-p+1], y_q[k-p+2], \cdots, y_q[k+1]\}$, and the reconstruction value of the system output $y[k+1]$ is calculated by

$$\bar{y}[k+1] = g_{k+1}(t_p).$$

Fig. 7 shows the updating strategy. In the case of $k \leq p$, $y_q[k-i]$ $(i = k, k+1, \cdots, p)$ is set as $y_q[k-i] := 0$. The signal $\bar{y}$ can be obtained by successively repeating the procedures.

In this way, however, $\bar{y}[k]$ and $\bar{y}[k+1]$ belong to different polynomials, and the smoothness of $\bar{y}$ cannot be guaranteed. In the following subsection, some constraint conditions are deduced to improve the accuracy and the smoothness of $\bar{y}$.

3.3 Constraint conditions

In order to improve the reconstruction accuracy and obtain a smooth signal $\bar{y}$, the model information is utilized to form several constraint conditions. As described in Section 2, the system output relative to the quantized output is always bounded by (9). Therefore, the reconstruction value $\bar{y}[k]$ should also be bounded by

$$|\bar{y}[k] - y_q[k]| \leq \frac{\Delta}{2}. \quad (14)$$

Note that the left part of (14) is convex to $\boldsymbol{\alpha}$.

Generally, the reconstruction signal $\bar{y}$ is preferred to be smooth since the true system output y is smooth due to the system dynamics. Therefore, the following two constraints can be applied as the conditions of (12).

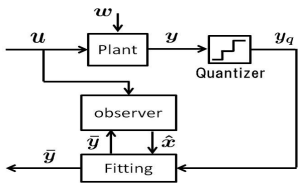

Fig. 8. Block diagram of the proposed approach, $\bar{y}$ is regarded as the reconstruction of y.

$$g_k(t_{p-1}) = \bar{y}[k-1], \quad (15)$$

$$\dot{g}_k(t_{p-1}) = \frac{1}{h}(\bar{y}[k] - \bar{y}[k-1]), \quad (16)$$

where $\dot{g}_k(t)$ is the slope of the polynomial (10), which is defined by

$$\dot{g}_k(t) = \alpha_1 + 2\alpha_2 t + \cdots + m\alpha_m t^{m-1}.$$

Equation (15) indicates that both $\bar{y}[k-1]$ and $\bar{y}[k]$ belong to $g_k(t)$, and equation (16) is a slope condition. These conditions imply that $\bar{y}[k-1]$ and $\bar{y}[k]$ are smoothly connected.

One problem of using conditions (15) and (16) is that the reconstruction error at last instant may be transmitted to next fitting procedure to deteriorate the reconstruction accuracy at next instant. In order to relax the problem, an improved solution based on the extended observer of the system (5) (6) is proposed. The observer is expressed as

$$\hat{\boldsymbol{x}}[k+1] = \boldsymbol{A}_d\hat{\boldsymbol{x}}[k] + \boldsymbol{B}_d u[k] + \boldsymbol{L}_d(\bar{y}[k] - \hat{y}[k]), \quad (17)$$

$$\hat{y}[k] = \boldsymbol{C}_d\hat{\boldsymbol{x}}[k], \quad (18)$$

where $\boldsymbol{L}_d \in \mathbb{R}^{(n+1)\times 1}$ is the observer gain which is designed to stabilize $\boldsymbol{A}_d - \boldsymbol{L}_d\boldsymbol{C}_d$. The conditions (15) (16) are then replaced by

$$g_k(t_{p-1}) = \hat{y}[k-1], \quad (19)$$

$$\dot{g}_k(t_{p-1}) = \frac{1}{h}(\hat{y}[k] - \hat{y}[k-1]), \quad (20)$$

For the implementation of real-time calculation, $\hat{y}[k]$ is computed via

$$\hat{y}[k] = \boldsymbol{C}_d\Big[\boldsymbol{A}_d\hat{\boldsymbol{x}}[k-1] + \boldsymbol{B}_d u[k-1] + \boldsymbol{L}_d\Big(\bar{y}[k-1] - \hat{y}[k-1]\Big)\Big]. \quad (21)$$

Note that the left hand sides of (19) and (20) are affine to $\boldsymbol{\alpha}$.

Taking the constraint conditions into account, the optimization problem for calculating the coefficient vector $\boldsymbol{\alpha}$ of the polynomial (10) is expressed as follows:

$$\begin{aligned} \underset{\boldsymbol{\alpha}}{\text{minimize}}: \quad & \|\boldsymbol{T}\boldsymbol{\alpha} - \boldsymbol{\beta}\|_2^2 + \eta\|\boldsymbol{\alpha}\|_1 \\ \text{subject to}: \quad & (14),\ (19),\ (20) \end{aligned} \quad (22)$$

The optimization problem (22) is a convex optimization problem. Note that the three constraint conditions are independent with each other, so the problem is feasible if the polynomial (10) has a degree not less than 2. The block diagram of the feedback control system is shown in Fig. 8.

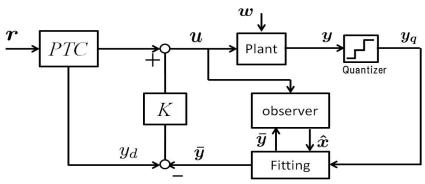

Fig. 9. Block diagram of linear stage control system.

4. SIMULATIONS

In this section, simulations are performed to evaluate the effectiveness of the proposed approach. The mathematical model (1) (2) and the controllers described in Section 2 are exploited for simulations. The sampling period is set as $T_s = 1$ms. The block diagram of the control system is shown in Fig. 9. In the figure, r denotes the trajectory, y_d is the desired system output. In order to evaluate the control performance and reconstruction performance, the following errors are defined:

$$e_q := y_q - y, \tag{23}$$

$$e_t := y_d - y, \tag{24}$$

$$e_r := \bar{y} - y. \tag{25}$$

e_q denotes the quantization error, e_t denotes the control error and e_r denotes the reconstruction error.

In the setup, the quantization step is set as 20μm, the degree of polynomial in (10) is set as $m = 3$, the number of quantized output used for fitting is $p + 1 = 15$, and the weight factor η is set as $\eta = 2 \times 10^{-3}$. the gain $\boldsymbol{L}_d$ of state estimator (17) is determined by placing the poles of the observer at [0.992 0.99 0.9881]. The input disturbance is set as a step signal. The trajectory reference is shown in Fig. 10. The C-code of solving the convex optimization problem (22) is generated by CVXGEN (Mattingley et al., 2010).

The simulation results are shown in Figs. 11 and 12. Fig. 11 shows the simulation results when quantized output is applied as feedback. In the figure, (a) shows the quantization error e_q, (b) shows the control error e_t and (c) shows the input signal. It is observed that the oscillation is raised in the settling motion area from $t = 3$s. The input behaves wildly due to the quantization error. Fig. 12 shows the simulation results when proposed approach is applied. In the figure, (a) shows the quantization error, (b) shows the control error, (c) is the reconstruction error, (d) shows the input and (e) shows the estimation of the input disturbance. It is obtained that the oscillation in the settling motion area is relaxed and the input also behaves softly. In addition, the input disturbance can be estimated after the convergence of extended observer. Therefore, it is observed that the proposed approach can improve the reconstruction performance.

5. EXPERIMENTS

This section demonstrates the application of the proposed polynomial fitting approach to the high-precision stage introduced in Section 2. The number of data used for polynomial fitting is set as $p + 1 = 15$, and the degree of polynomial is set as $m = 3$. The weight factor η is

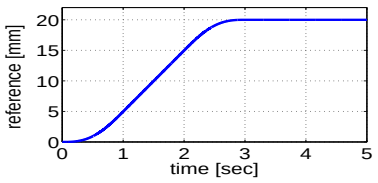

Fig. 10. Reference of simulation.

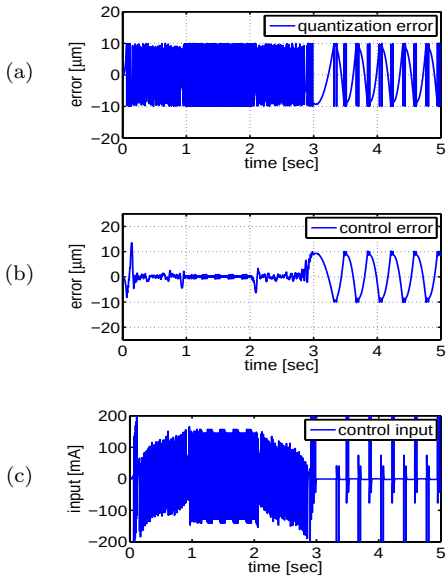

Fig. 11. Simulation results when quantized output is used as feedback (conventional method).

properly chosen as $\eta = 2 \times 10^{-3}$, and the quantization step is set as $\Delta = 20\mu$m. The gain $\boldsymbol{L}_d$ of state estimator (17) is determined by placing the poles of the observer at $[0.5335, 0.6242, 0.7304]$, which results in the observer bandwidth as 20Hz. By this setting, the average computational time of solving the convex optimization problem (22) is about 3 ms. The sampling period is set as $T_s = 5$ms to allow enough time for solving (22).

The position and velocity reference of the linear stage is also given as Fig. 5. The experimental results are shown in Fig. 13. Fig. 13(a) shows the comparison of the desired reference y_d, the controlled output y and the reconstructed output $\bar{y}$. The position tracking error and the reconstructed error are shown in Fig. 13(b), (c). It is observed that the reconstruction error is much smaller than the quantization error. Moreover, the high-order vibration is also suppressed, especially in the settling motion area. Fig. 13(d) shows the control input and the estimated disturbance. It is observed that the control input is smoother compared to Fig. 6(d). Therefore, the effectiveness of the proposed method is verified.

6. CONCLUSION

In this paper, a polynomial fitting approach is proposed to reconstruct the quantized output of motion systems. In order to properly fit the complex output signals as well as the simple output signals, ℓ_1-norm regularization method is exploited to automatically determine the degree

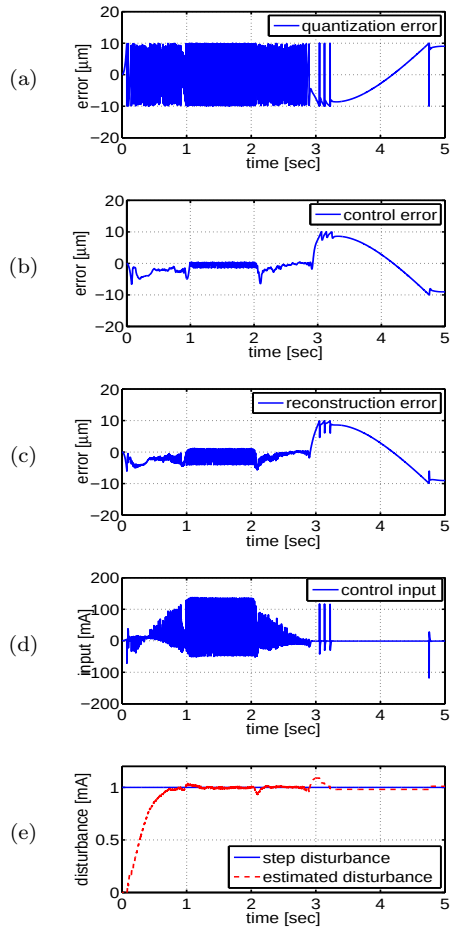

Fig. 12. Simulation results when reconstructed output is used as feedback (proposed method).

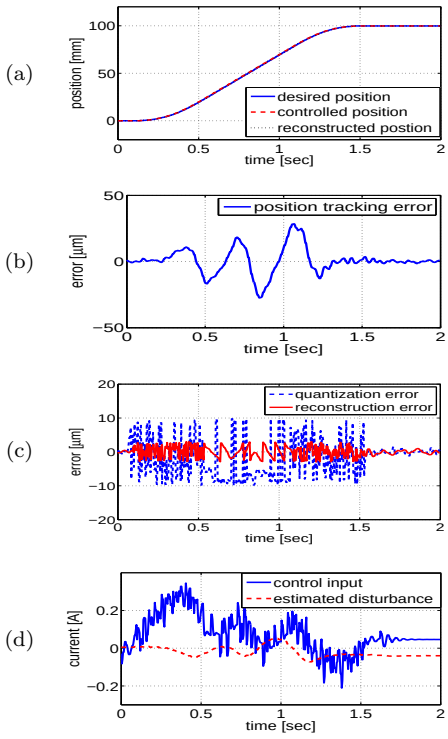

Fig. 13. Experimental results of the proposed method. (a) is the comparison of the desired reference y_d, real output y and the reconstructed output $\bar{y}$, (b) shows the position tracking error. (c) shows the comparison of the quantization error and the reconstruction error, and (d) is the input and the estimated disturbance.

of the polynomial. In addition, some constraint conditions deduced from the feature of quantization and the system model are utilized to improve the accuracy of reconstruction. The approach is also applied to a high-precision linear stage with an optical encoder that is low-resolution. The simulation and experimental results demonstrate the effectiveness of the proposed method.

REFERENCES

D. Luong-Van, M. Tordon, and J. Katupitiya. (2004). Covariance profiling for an adaptive Kalman filter to suppress sensor quantization effects. *Proceedings 43rd IEEE Conference on Decision and Control*, 2680–2685.

F. Franklin, J. D. Powell, M. Workman. (1998). *Digital control of dynamic systems.* 3rd edition, Addison-Wesley.

H. Fujimoto, Y. Hori, and A. Kawamura. (2001). Perfect tracking control based on multirate feedforward control with generalized sampling periods. *IEEE Trans. Industrial Electronics*, Vol. 48, No. 3, pp. 636–644.

H. Zhu, and T. Sugie. (2012). Velocity estimation of motion systems based on low-resolution encoders. *Trans. of the ASME, Journal of Dynamic Systems, Measurement and Control*, unpublished.

J. Mattingley, Y. Wang, and S. Boyd. (2010). Code generation for moving horizon control. *Proceedings IEEE Multi-Conference on Systems and Control*, pp. 985–992, Yokohama, Japan.

J. Sur, and B. E. Paden. (1998). State observer for linear time-invariant systems with quantized output. *Journal of Dynamic Systems, Measurement, and Control*, Vol. 120, pp. 423–426.

J. Zhang, and M. Fu. (2008). A reset state estimator for linear systems to suppress sensor quantization effects. Proc. 17th IFAC World Congress, pp. 9254–9259.

M. Hirata, and T. Kidokoro. (2009). Servo performance enhancement of motion system via a quantization error estimation method–introduction to nanoscle servo control. *IEEE Trans. Ind. Electron.*, Vol. 56, No. 10, pp. 3817–3824.

P.R. Bélanger, P. Dobrovolny, A. Helmy, and X. Zhang. (1998). Estimation of angular velocity and acceleration from shaft-encoder measurements. *The International Journal of Robotics Research*, Vol. 17, No. 11, pp. 1225–1233.

R.J.E. Merry, M.J.G. van de Molengraft, and M. Steinbuch. (2010). Velocity and acceleration estimation for optical incremental encoders. *Mechatronics 20*, pp. 20–26.

S. Devasia, E. Eleftheriou and M.S.O. Reza. (2007) A survey of control issues in nanopositioning. *IEEE Trans. Control Syst. Technol.*, Vol. 15, No. 5, pp. 802–823.

T.R. Tesch, and R.D. Lorenz. (2008). Disturbance torque and motion state estimation with low-resolution position interfaces using heterodyning observers. *IEEE Trans. on Ind. Appl.*, Vol. 44, No. 1, pp. 124–134.